Reactions of Group IV Metal Atoms with Water Molecules. Matrix Isolation FTIR and Theoretical Studies

4 AUTHORS, INCLUDING:

Mingfei Zhou
Fudan University

259 PUBLICATIONS **5,074** CITATIONS

SEE PROFILE

Jian Dong
Zhejiang University of Technology

30 PUBLICATIONS **382** CITATIONS

SEE PROFILE

Reactions of Group IV Metal Atoms with Water Molecules. Matrix Isolation FTIR and Theoretical Studies

Mingfei Zhou,* Luning Zhang, Jian Dong, and Qizong Qin

Contribution from the Laser Chemistry Institute, Department of Chemistry, Fudan University, Shanghai, People's Republic of China

Received June 9, 2000

Abstract: Laser-ablated group IV metal atoms have been co-deposited at 11 K with water molecules in excess argon. The metal atoms reacted with water to form the insertion product HMOH and $H_2M(OH)_2$ (M = Ti, Zr, Hf) molecules spontaneously. Photolysis of the HTiOH species produced the H_2TiO molecule as well as the TiO monoxide. In the cases of Zr and Hf, however, the H_2ZrO and H_2HfO molecules were produced on annealing, and the H_2 elimination process was not observed on photolysis. In addition, the HMO species were also observed and identified. The aforementioned species were identified via isotopic substitutions as well as theoretical frequency calculations. Qualitative analysis of the possible reaction paths leading to the observed products is proposed.

Introduction

The interactions of transition metals with small molecules are of chemical interest as such reactions may play important roles in catalytic and chemisorption processes. Recent studies of transition metal atoms with small molecules have provided insight into the activation of bonds such as H−H,[1] C−O,[2] and N−O.[3] There are several reports on the reactions of transition metal atoms with water molecules. Liu and Parson reported that atomic Sc reacted with water to give ScO in the gas phase.[4] Using the matrix isolation infrared absorption method, Kauffman et al. showed that thermal Sc, Ti, and V atoms could react with water to form the insertion products spontaneously, while the metal monoxides were formed on photolysis, but later transition metal atoms formed adducts with water, which were rearranged to the insertion molecules on photolysis.[5,6] To our knowledge, there is no report on the reactions of the second- and third-row transition metals with water.

The reactions of transition metal cations and water have received much attention recently. The $M^+ + H_2O \rightarrow MO^+ + H_2$ and its reverse reactions have been studied both experimentally[7−11] and theoretically.[12−19] The different gas-phase

reactivity depending on the spin, electron configuration, and spin−orbital level has been discussed. These results showed that earlier transition metal cations (Sc^+, Ti^+, and V^+) are more reactive than their oxides, and the formation of the low-lying state $MO^+ + H_2$ is the only exothermic process.[7−9,17,18] It is of great interest to compare the chemistry of transition metal cations and neutral atoms.

Recently, we have performed a matrix isolation FTIR and theoretical study of reactions of laser-ablated Sc with water.[20] The difference between laser-ablated and thermal evaporated Sc atom reactions is the observation of HScO and ScOH molecules with laser ablation. In this paper, we present a combined matrix isolation FTIR spectroscopic and theoretical investigation on the reactions of laser-ablated group IV metal atoms with water molecules.

Experimental and Theoretical Methods

The experimental setup for pulsed laser ablation and matrix infrared spectroscopic investigation has been described previously[21] and is similar to the technique employed by the Andrews group.[22] The 1064-nm Nd:YAG laser fundamental (Spectra Physics, DCR 150, 20 Hz repetition rate and 8 ns pulse width) was focused onto the rotating metal target through a hole in a CsI window, and the ablated metal atoms were co-deposited with H_2O in excess argon onto a 11 K CsI window, which was mounted on a cold tip of a closed-cycle helium refrigerator (Air Products, Model CSW202), for 1 h at a rate of

* Corresponding author. E-mail: mfzhou@srcap.stc.sh.cn. Fax: 0086-21-65102777.

(1) See, for example: Chertihin, G. V.; Andrews, L. *J. Am. Chem. Soc.* **1994,** *116,* 8322; **1995,** *117,* 6402.

(2) See, for example: Zhou, M. F.; Andrews, L. *J. Am. Chem. Soc.* **1998,** *120,* 13230; **2000,** *122,* 1531.

(3) See, for example: Kushto, G. P.; Zhou, M. F.; Andrews, L.; Bauschlicher, C. W., Jr. *J. Phys. Chem. A* **1999,** *103,* 1115. Zhou, M. F.; Andrews, L. *J. Phys. Chem. A* **1998,** *102,* 7452.

(4) Liu, K.; Parson, J. M. *J. Chem. Phys.* **1978,** *68,* 1794.

(5) Kauffman, J. W.; Hauge, R. H.; Margrave, J. L. *J. Phys. Chem.* **1985,** *89,* 3541.

(6) Kauffman, J. W.; Hauge, R. H.; Margrave, J. L. *J. Phys. Chem.* **1985,** *89,* 3547.

(7) Clemmer, D. E.; Aristov, N.; Armentrout, P. B. *J. Phys. Chem.* **1993,** *97,* 544.

(8) Chen, Y. M.; Clemmer, D. E.; Armentrout, P. B. *J. Phys. Chem.* **1994,** *98,* 11490.

(9) Guo, B. C.; Kerns, K. P.; Castleman, A. W. *J. Phys. Chem.* **1992,** *96,* 4879.

(10) Ryan, M. F.; Fiedler, A.; Schroder, D.; Schwarz, H. *J. Am. Chem. Soc.* **1995,** *117,* 2033.

(11) Schroder, D.; Fiedler, A.; Ryan, M. F.; Schwarz, H. *J. Phys. Chem.* **1994,** *98,* 68.

(12) Clemmer, D. E.; Chen, Y. M.; Khan, F. A.; Armentrout, P. B. *J. Phys. Chem.* **1994,** *98,* 6522.

(13) Tilson, J. L.; Harrison, J. F. *J. Phys. Chem.* **1991,** *95,* 5097.

(14) Fiedler, A.; Schroder, D.; Shaik, S.; Schwarz, H. *J. Am. Chem. Soc.* **1994,** *116,* 10734.

(15) Danovich, D.; Shaik, S. *J. Am. Chem. Soc.* **1997,** *119,* 1773.

(16) Ye, S. *THEOCHEM* **1997,** *417,* 157.

(17) Irigoras, A.; Fowler, J. E.; Ugalde, J. M. *J. Phys. Chem. A* **1998,** *102,* 293.
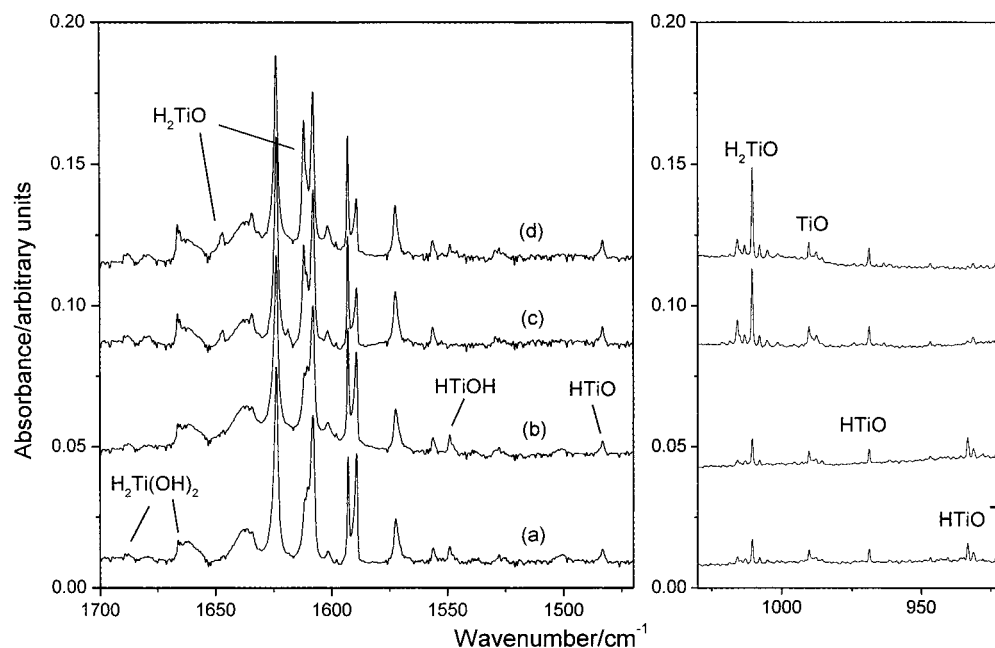
(18) Irigoras, A.; Fowler, J. E.; Ugalde, J. M. *J. Am. Chem. Soc.* **1999,** *121,* 574.

(19) Irigoras, A.; Fowler, J. E.; Ugalde, J. M. *J. Am. Chem. Soc.* **1999,** *121,* 8549.

(20) Zhang, L. N.; Dong, J.; Zhou, M. F. *J. Phys. Chem. A,* to be published.

(21) Chen, M. H.; Wang, X. F.; Zhang, L. N.; Yu, M.; Qin, Q. Z. *Chem. Phys.* **1999,** *242,* 81.

(22) Burkholder, T. R.; Andrews, L. *J. Chem. Phys.* **1991,** *95,* 8697.

Figure 1. Infrared spectra in the 1700−1460 and 1030−920 cm^{-1} regions from co-deposition of laser-ablated Ti with 0.2% water in argon: (a) 1 h sample deposition, (b) 25 K annealing, (c) 20 min broadband photolysis, and (d) annealing to 30 K.

2−4 mmol/h. Typically, 5−10 mJ/pulse laser power was used. H_2O, $H_2^{18}O$(96% ^{18}O), and D_2O were subjected to several freeze−pump−thaw cycles before use. Infrared spectra were recorded on a Bruker IFS113V spectrometer at 0.5 cm^{-1} resolution using a DTGS detector. Matrix samples were annealed at different temperatures, and selected samples were subjected to broadband photolysis using a high-pressure mercury lamp.

Quantum chemical calculations were performed using the Gaussian 98 program.[23] The three-parameter hybrid functional according to Becke with additional correlation corrections due to Lee, Yang, and Parr was utilized (B3LYP).[24,25] Recent calculations have shown that this hybrid functional can provide accurate results for the geometries and vibrational frequencies for transition metal-containing compounds.[17−19,26,27] The 6-311++G(d,p) basis sets were used for H and O atoms, the all-electron basis sets of Wachter−Hay as modified by Gaussian were used for Ti atom, and the Los Alamos ECP plus DZ basis sets were used for Zr and Hf atoms.[28−30] These ECPs incorporate Darwin relativistic effects into the potentials. Recent reports have shown that density functional theoretical calculations using similar basis sets on O or C atoms and effective core potentials on metal atoms predicted the geometries, vibrational frequencies, and energetics of second- and third-row transition metal compounds reasonably well.[31] Reactants, various

Table 1. Infrared Absorptions (cm^{-1}) from Co-deposition of Laser-Ablated Ti with Water in Excess Argon

H_2O	D_2O	$H_2^{18}O$	assignment
1688.3		1687.3	$H_2Ti(OH)_2$ sym-TiH_2
1666.2		1665.8	$H_2Ti(OH)_2$ asym-TiH_2
1646.8		1645.4	H_2TiO sym-TiH_2
1634.3			$HTi(OH)_3$ Ti−H
1611.9	1168.2	1611.3	H_2TiO asym-TiH_2
1549.1		1549.1	HTiOH Ti−H
1483.3	1071.1	1482.8	HTiO Ti−H
1341.8	978.3		HTiO$^-$ Ti−H
1015.8			$H_2^{46}TiO$
1013.0			$H_2^{47}TiO$
1010.5	1009.6	968.8	$H_2^{48}TiO$ Ti−O
1008.0			$H_2^{49}TiO$
1005.3			$H_2^{50}TiO$
990.3	990.3	948.4	TiO
974.2			$H^{46}TiO$
971.5			$H^{47}TiO$
968.8	967.9	928.1	$H^{48}TiO$ Ti−O
966.3			$H^{49}TiO$
963.5			$H^{50}TiO$
933.4	931.1	895.8	HTiO$^-$ Ti−O
844.3			$HTi(OH)_3$ Ti−OH
805.5			$H_2Ti(OH)_2$ asym-Ti−$(OH)_2$
775.5			$H_2Ti(OH)_2$ symm-Ti−$(OH)_2$

possible transition states, intermediates, and products were optimized. The vibrational frequencies were calculated with analytic second derivatives, and zero-point vibrational energies (ZPVE) were derived. Single-point CCSD(t) calculations have been carried out at the B3LYP equilibrium geometries with the same basis sets for selected systems.

Results and Discussion

Infrared Spectra. Experiments were done with different water concentrations ranging from 0.2% to 0.5% in argon. Typical infrared spectra for the reactions of laser-ablated Ti, Zr, and Hf atoms with 0.2% water molecules in argon in the metal hydride and metal oxide stretching vibrational frequency regions are shown in Figures 1−3, respectively, and the product absorptions are listed in Tables 1−3. The stepwise annealing

(23) Frisch, M. J.; Trucks, G. W.; Schlegel, H. B.; Scuseria, G. E.; Robb, M. A.; Cheeseman, J. R.; Zakrzewski, V. G.; Montgomery, J. A., Jr.; Stratmann, R. E.; Burant, J. C.; Dapprich, S.; Millam, J. M.; Daniels, A. D.; Kudin, K. N.; Strain, M. C.; Farkas, O.; Tomasi, J.; Barone, V.; Cossi, M.; Cammi, R.; Mennucci, B.; Pomelli, C.; Adamo, C.; Clifford, S.; Ochterski, J.; Petersson, G. A.; Ayala, P. Y.; Cui, Q.; Morokuma, K.; Malick, D. K.; Rabuck, A. D.; Raghavachari, K.; Foresman, J. B.; Cioslowski, J.; Ortiz, J. V.; Baboul, A. G.; Stefanov, B. B.; Liu, G.; Liashenko, A.; Piskorz, P.; Komaromi, I.; Gomperts, R.; Martin, R. L.; Fox, D. J.; Keith, T.; Al-Laham, M. A.; Peng, C. Y.; Nanayakkara, A.; Gonzalez, C.; Challacombe, M.; Gill, P. M. W.; Johnson, B.; Chen, W.; Wong, M. W.; Andres, J. L.; Gonzalez, C.; Head-Gordon, M.; Replogle, E. S.; Pople, J. A. *Gaussian 98*, Revision A.7; Gaussian, Inc.: Pittsburgh, PA, 1998.

(24) Becke, A. D. *J. Chem. Phys.* **1993**, *98*, 5648.

(25) Lee, C.; Yang, E.; Parr, R. G. *Phys. Rev. B* **1988**, *37*, 785.

(26) Bauschlicher, C. W., Jr.; Ricca, A.; Partridge, H.; Langhoff, S. R. In *Recent Advances in Density Functional Theory*; Chong, D.P., Ed.; World Scientific Publishing: Singapore, 1997; Part II.

(27) Bytheway, I.; Wong, M. W. *Chem. Phys. Lett.* **1998**, *282*, 219.

(28) McLean, A. D.; Chandler, G. S. *J. Chem. Phys.* **1980**, *72*, 5639. Krishnan, R.; Binkley, J. S.; Seeger, R.; Pople, J. A. *J. Chem. Phys.* **1980**, *72*, 650.

(29) Wachter, J. H. *J. Chem. Phys.* **1970**, *52*, 1033. Hay, P. J. *J. Chem. Phys.* **1977**, *66*, 4377.

(30) Hay, P. J.; Wadt, W. R. *J. Chem. Phys.* **1985**, *82*, 299.

(31) See, for example: Andrews, L.; Zhou, M. F.; Chertihin, G. V.; Bauschlicher, C. W., Jr. *J. Phys. Chem. A* **1999**, *103*, 6525. Zhou, M. F.; Andrews, L. *J. Phys. Chem. A* **1999**, *103*, 7763.
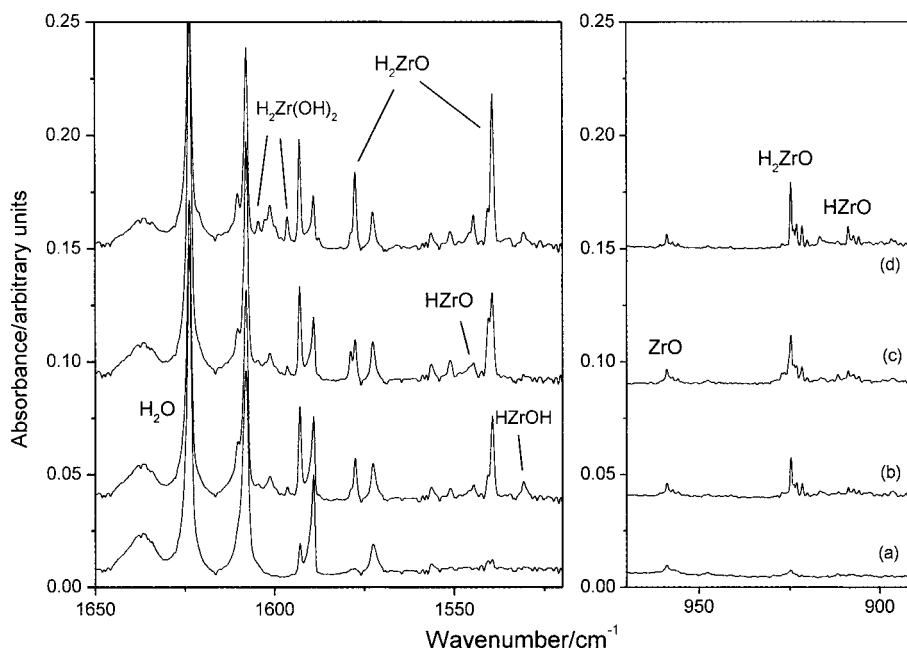
Figure 2. Infrared spectra in the 1650−1520 and 970−890 cm^{-1} regions from co-deposition of laser-ablated Zr with 0.2% water in argon: (a) 1 h sample deposition, (b) 25 K annealing, (c) 20 min broadband photolysis, and (d) annealing to 30 K.
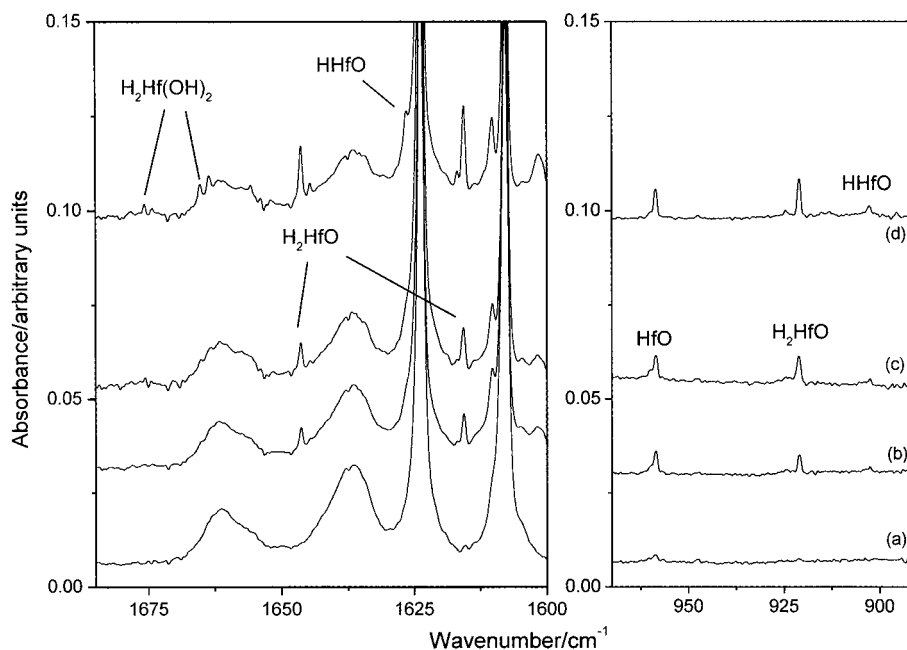
Figure 3. Infrared spectra in the 1685−1600 and 970−890 cm^{-1} regions from co-deposition of laser-ablated Hf with 0.2% water in argon: (a) 1 h sample deposition, (b) 25 K annealing, (c) 20 min broadband photolysis, and (d) annealing to 30 K.

and photolysis behavior of these product absorptions is also shown in the figures and will be discussed below. D$_2$O and H$_2$^{18}O samples were employed for product identification through isotopic shift and splitting, and the representative spectra with mixed H$_2$O + HDO + D$_2$O and H$_2$^{16}O + H$_2$^{18}O in selected regions are shown in Figures 4−7, respectively.

Calculation Results. The energy differences between the ^{3}F ground state and the ^{1}D first singlet excited state of metal atoms are listed in Table 4. The B3LYP results are slightly overestimated, and the CCSD(t) results are closer to the experimental values.[32] Calculation results on monoxides are listed in Table 5. CCSD(t) calculations predicted the ground states correctly, but B3LYP calculations predicted the $^3\Delta$ state to be the ground state for ZrO, which is in error.[33]

Calculations were done on two [M,O,H] isomers, namely HMO and MOH (M = Ti, Zr, Hf). The calculated geometric parameters and relative stability are shown in Figure 8, and the vibrational frequencies and intensities are listed in Table 6. All three HMO molecules in this family were predicted to have doublet ground states with bent geometry and are more stable than the MOH isomers.

Calculations were also done for two isomers of MH$_2$O on both singlet and triplet potential energy surfaces, namely, the inserted HMOH molecules and the H$_2$MO molecules. The

(32) Moore, C. E. *Atomic Energy Levels*; National Bureau of Standards: Washington, DC, 1959.
(33) Hammer, P. D.; Davis, S. P. *Astrophys. J.* **1980**, *237*, L51. Langhoff, S. R.; Bauschlicher, C. W., Jr. *J. Chem. Phys.* **1988**, *89*, 2160.

Table 2. Infrared Absorptions (cm^{-1}) from Co-deposition of Laser-Ablated Zr Atoms with Water in Excess Argon

H_2O	D_2O	$H_2^{18}O$	assignment
1604.6			$H_2Zr(OH)_2$ sym-ZrH_2
1596.5			$H_2Zr(OH)_2$ asym-ZrH_2
1577.6	1130.3	1577.6	H_2ZrO sym-ZrH_2
1544.7	1110.1	1544.7	$HZrO$ Zr$-$H
1539.4	1107.8	1539.5	H_2ZrO asym-ZrH_2
1530.9	1098.2	1530.5	$HZrOH$ Zr$-$H
958.9	958.9	912.8	^{90}ZrO
957.3	957.3	911.2	^{92}ZrO
955.8	955.8	909.7	^{94}ZrO
924.7	922.4	881.2	$H_2^{90}ZrO$ Zr$-$O
923.9	921.6	880.4	$H_2^{91}ZrO$
923.1	920.8	879.5	$H_2^{92}ZrO$
921.6	919.3	877.9	$H_2^{94}ZrO$
908.8	907.4	865.7	$H^{90}ZrO$ Zr$-$O
908.1		865.0	$H^{91}ZrO$
907.3	906.0	864.2	$H^{92}ZrO$
905.8	904.4	862.7	$H^{94}ZrO$
707.3	680.7		$H_2Zr(OH)_2$ asym-Zr$-(OH)_2$
660.1	635.4		$H_2Zr(OH)_2$ sym-Zr$-(OH)_2$

Table 3. Infrared Absorptions (cm^{-1}) from Co-deposition of Laser-Ablated Hf Atoms with Water in Excess Argon

H_2O	D_2O	$H_2^{18}O$	assignment
1675.8	1241.5	1675.8	$H_2Hf(OH)_2$ sym-HfH_2
1665.3	1233.0	1665.3	$H_2Hf(OH)_2$ asym-HfH_2
1626.5		1626.5	$HHfO$ Hf$-$H
1646.4		1646.4	H_2HfO sym-HfH_2
1615.6	1158.1	1615.6	H_2HfO asym-HfH_2
958.7	958.7	908.6	HfO
921.0	918.7	873.8	H_2HfO Hf$-$O
902.9	900.9	855.6	$HHfO$ Hf$-$O
690.7	662.4		$H_2Hf(OH)_2$ asym-Hf$-(OH)_2$
660.4	636.1		$H_2Hf(OH)_2$ sym-Hf$-(OH)_2$

Table 4. Relative Energies (kcal/mol) for the ^3F and ^1D States of Ti, Zr, and Hf

	B3LYP	CCSD(t)	exptl
Ti	34.8	27.1	20.1
Zr	26.3	7.5	12.5
Hf	22.7	15.6	8.3

Table 5. Calculated Bond Lengths (Å), Relative Energies (kcal/mol), Vibrational Frequencies (cm^{-1}), and Intensities (km/mol) for the $^3\Delta$ and $^1\Sigma^+$ States of TiO, ZrO, and HfO

	relative energy		bond length	frequency (intensity)
molecule	B3LYP	CCSD(t)		
TiO ($^3\Delta$)	0	0	1.612	1043 (220)
TiO($^1\Sigma^+$)	+28.8	+17.0	1.587	1079 (273)
ZrO ($^1\Sigma^+$)	0	0	1.745	976 (164)
ZrO($^3\Delta$)	−8.5	+7.1	1.763	930 (172)
HfO($^1\Sigma^+$)	0	0	1.731	969 (120)
HfO($^3\Delta$)	+23.3	+36.6	1.752	912 (132)

geometric parameters and relative stability are shown in Figure 9, and the vibrational frequencies and intensities are listed in Table 7. At both B3LYP and CCSD(t) levels of theory, the H_2MO isomers were predicted to have $^1A'$ ground state with nonplanar geometry and are more stable than the inserted HMOH molecules. The inserted HTiOH and HZrOH molecules were calculated to have $^3A''$ ground states, and HHfOH a $^1A'$ ground state. Our calculation results on H_2TiO and HTiOH molecules are in reasonable agreement with previous ab initio molecular orbital calculations reported by Kudo and Gordon.[34] Their calculations also predicted that the singlet ground-state

(34) Kudo, T.; Gordon, M. S. *J. Phys. Chem. A* **1998**, *102*, 6967.
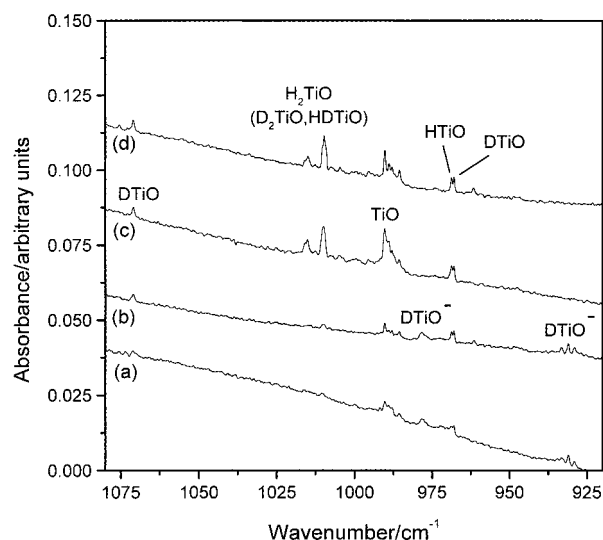
Figure 4. Infrared spectra in the 1080−920 cm^{-1} region from co-deposition of laser-ablated Ti with 0.4% (H_2O + HDO + D_2O) in argon: (a) 1 h sample deposition, (b) 25 K annealing, (c) 20 min broadband photolysis, and (d) annealing to 30 K.

H_2TiO molecule is slightly lower in energy than the triplet ground-state HTiOH molecule.

Similar B3LYP calculations were performed on $H_2M(OH)_2$ (M = Ti, Zr, Hf) and $HTi(OH)_3$ molecules, as shown in Figure 10. The $H_2M(OH)_2$ molecules were predicted to have $^1A_1$ ground state and C_{2v} symmetry with the MH_2 plane perpendicular to the $M(OH)_2$ plane.

MO. The bands at 990.3, 987.8, and 985.5 cm^{-1} showed no deuterium isotopic shift and are assigned to the TiO molecule in different trapping sites in solid argon based on a recent matrix isolation study of the Ti + O_2 reaction.[35] In a previous study on thermal Ti atom and water reaction,[6] a 1010 cm^{-1} band was assigned to the TiO molecule; this band will be reassigned to the H_2TiO molecule, as will be discussed below. At the B3LYP/6-311+G(d) level, the TiO molecule was predicted to have a $^3\Delta$ ground state with vibrational fundamental at 1043 cm^{-1}.

The 959.0 cm^{-1} band in the Zr + H_2O experiment and the 958.7 cm^{-1} band in the Hf + H_2O experiment are assigned to the ZrO and HfO molecules on the basis of isotopic shifts and previous works.[35−37]

HMO. The 1483.1 and 968.7 cm^{-1} bands in the Ti + H_2O experiments went together through all experiments, suggesting different modes of the same molecule. The upper band showed a very small shift with $H_2^{18}O$ sample and was shifted to 1071.0 cm^{-1} when the D_2O sample was used. The H/D isotopic ratio of 1.3848 is characteristic of a Ti$-$H stretching vibration. The lower band exhibited the characteristic titanium isotopic distribution for a single Ti atom;[38] it shows a very small (0.9 cm^{-1}) deuterium isotopic shift but was shifted to 928.1 cm^{-1} with the $H_2^{18}O$ sample. The 16/18 ratio of 1.0437 indicates that this band is mainly due to a Ti$-$O stretching vibration. These two bands are assigned to the HTiO molecule. DFT calculations predicted the HTiO molecule to have a $^2A''$ ground state with Ti$-$H and Ti$-$O stretching vibrations at 1563 and 1034 cm^{-1}.

(35) Chertihin, G. V.; Andrews, L. *J. Phys. Chem.* **1995**, *99*, 6356.
(36) McIntyre, N. S.; Rhompson, K. R.; Weltner, W., Jr. *J. Phys. Chem.* **1971**, *75*, 3243.
(37) Simard, B.; Mitchell, S. A.; Humphries, M. R.; Hackett, P. A. *J. Mol. Spectrosc.* **1988**, *129*, 186.
(38) *CRC handbook*; CRC Press: Boca Raton, FL, 1985. ^{46}Ti, 8.0%; ^{47}Ti, 7.5%; ^{48}Ti, 73.7%; ^{49}Ti, 5.5%; ^{50}Ti, 5.3%; ^{90}Zr, 51.4%; ^{91}Zr, 11.2%; ^{92}Zr, 17.1%; ^{94}Zr, 17.5%; ^{96}Zr, 2.8%.
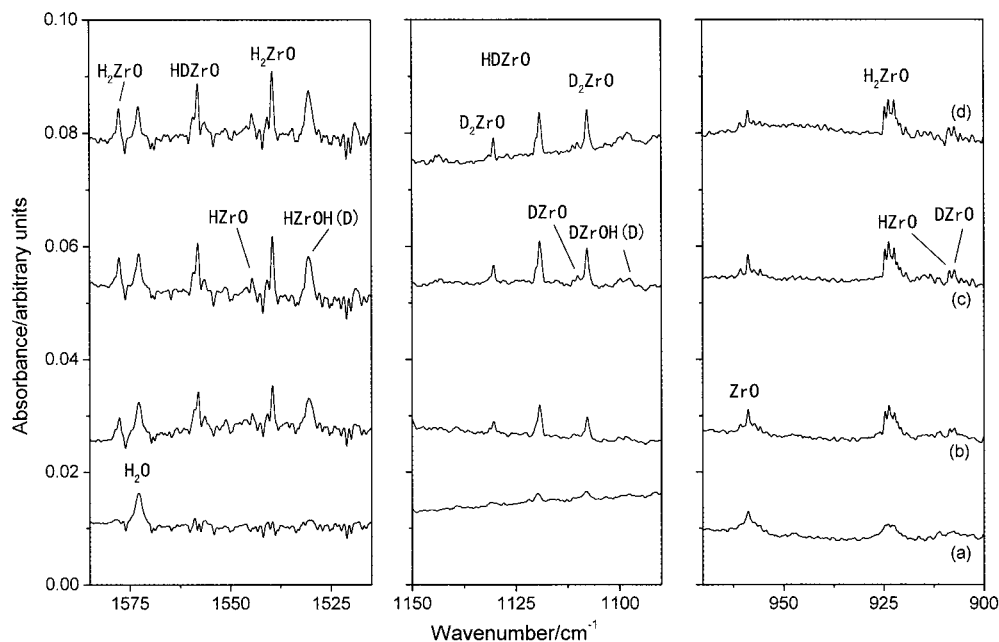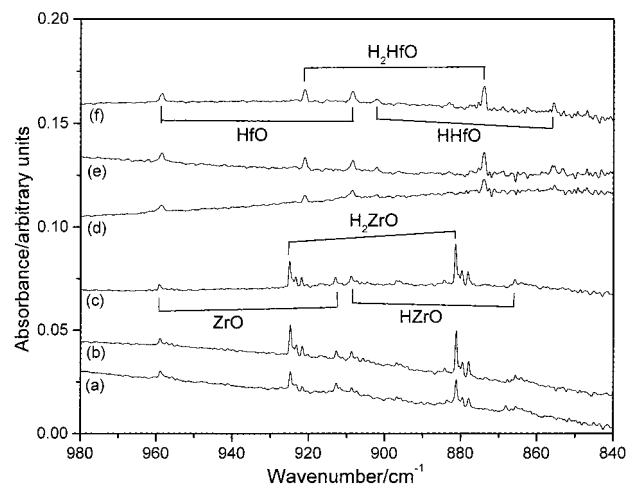
Figure 5. Infrared spectra in the 1585−1515, 1150−1090, and 970−900 cm^{-1} regions from co-deposition of laser-ablated Zr with 0.4% (H$_2$O + HDO + D$_2$O) in argon: (a) 1 h sample deposition, (b) 25 K annealing, (c) 20 min broadband photolysis, and (d) annealing to 30 K.
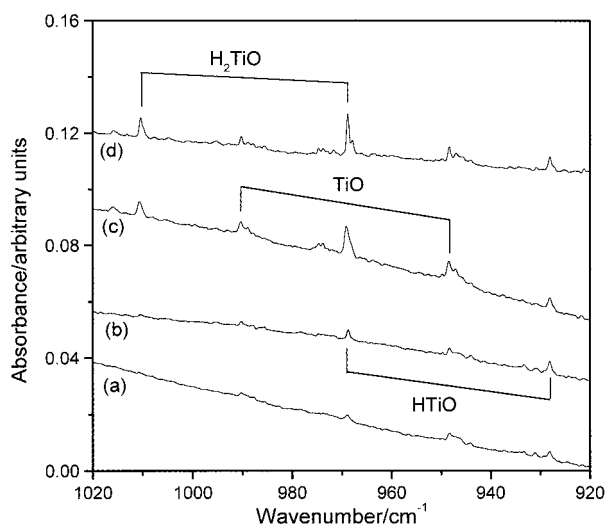

Figure 6. Infrared spectra in the 1020−920 cm^{-1} region from co-deposition of laser-ablated Ti with 0.4% (H$_2$^{16}O + H$_2$^{18}O) in argon: (a) 1 h sample deposition, (b) 25 K annealing, (c) 20 min broadband photolysis, and (d) annealing to 30 K.

Figure 7. Infrared spectra in the 980−840 cm^{-1} region from co-deposition of laser-ablated Zr and Hf with 0.4% (H$_2$^{16}O + H$_2$^{18}O) in argon: (a) Zr, 1 h sample deposition, (b) Zr, 25 K annealing, (c) Zr, annealing to 30 K, (d) Hf, 1 h sample deposition, (e) Hf, 25 K annealing, and (f) Hf, annealing to 30 K.

In the Zr + H$_2$O experiments, bands at 908.8, 908.1, 907.3, and 905.8 cm^{-1} exhibited the intensity distribution for natural abundance Zr isotopes.[38] In the reactions of Zr with a H$_2$O + HDO + D$_2$O mixture, these bands split into very closely spaced doublets. In the reactions of Zr with a H$_2$^{16}O + H$_2$^{18}O mixture, doublets were also observed, but with much greater separations. The metal, deuterium, and oxygen isotopic shifts indicate the presence of only one metal atom, one oxygen atom, and one hydrogen atom. The 1544.7 cm^{-1} band exhibited the same annealing and photolysis behavior as the 908.8 cm^{-1} band; the deuterium isotopic shift indicates a Zr−H stretching vibration. Accordingly, these bands are assigned to the Zr−H and Zr−O stretching vibrations of the HZrO molecule. As with HTiO, B3LYP calculations on the HZrO predicted a bent structure. Frequency calculations on the ground ^{2}A′ state produced vibrational modes at 1634 and 937 cm^{-1}, which require scaling factors of 0.945 and 0.970 to fit the observed values.

Absorptions at 1626.5 and 902.9 cm^{-1} in the Hf + H$_2$O experiments are assigned to the Hf−H and Hf−O stretching vibrations of the HHfO molecule following the examples of HTiO and HZrO. B3LYP calculations predicted the two vibrational modes at 1683 and 933 cm^{-1} for the bent ^{2}A′ ground-state HHfO molecule.

H$_2$MO. The 1010.5 cm^{-1} band was weak on sample deposition but was markedly increased on broadband photolysis. The Ti isotopic splittings were clearly resolved, which indicate that only one Ti atom is involved in this vibration. This band shifted to 968.8 cm^{-1} for H$_2$^{18}O sample and gave a ^{16}O/^{18}O isotopic ratio of 1.0429. The Ti and oxygen-18 isotopic shifts suggest that it is due to a terminal Ti−O stretching vibration. This band has been assigned to the TiO molecule in previous thermal Ti atom reactions with water in solid argon on the basis of the metal and oxygen isotopic shifts and the absence of a deuterium shift.[6] However, in our experiments with 0.5 cm^{-1} resolution, this band does show a very small deuterium shift (0.9 cm^{-1}),
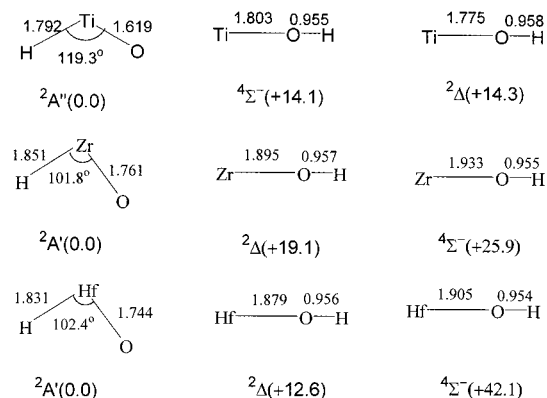
Figure 8. B3LYP-calculated geometric parameters (bond lengths in angstroms; bond angles in degrees) and relative stability (kilocalories per mole) of the HMO and MOH isomers.
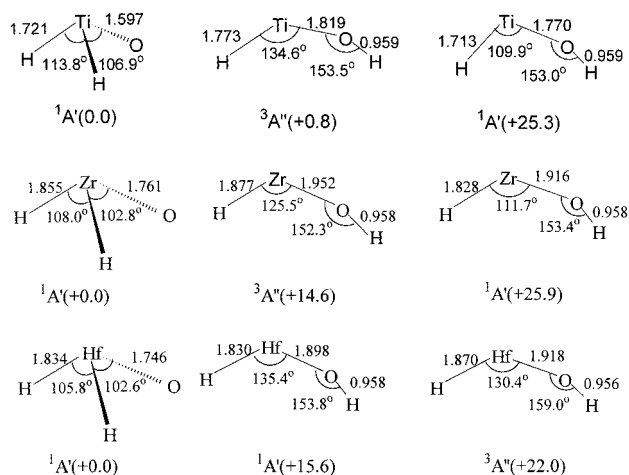
Table 6. Calculated Vibrational Frequencies (cm^{-1}) and Intensities (km/mol) for the Structures Described in Figure 8

molecule	frequency (intensity)
HTiO (^{2}A$''$)	1563 (289), 1034 (260), 412 (180)
TiOH ($^4\Sigma^-$)	3990 (279), 743 (132), 169 (114)
TiOH ($^2\Delta$)	3923 (258), 718 (68), 111 (95)
HZrO (^{2}A$'$)	1634 (323), 937 (204), 534 (51)
ZrOH ($^4\Sigma^-$)	3984 (283), 693 (100), 218 (232)
ZrOH ($^2\Delta$)	3958 (406), 738 (67), 298 (220)
HHfO (^{2}A$'$)	1683 (170), 933 (156), 541 (39)
HfOH ($^4\Sigma^-$)	4001 (257), 685 (79), 194 (193)
HfOH ($^2\Delta$)	3976 (310), 720 (54), 280 (122)

and a broad band centered at 1010.0 cm^{-1} was observed in the mixed $H_2O + HDO + D_2O$ experiments. In concert, two bands at 1646.8 and 1611.9 cm^{-1} tracked with the 1010.5 cm^{-1} band, suggesting different modes of the same molecule. These two bands exhibited very small shifts for the $H_2^{18}O$ sample. The 1611.9 cm^{-1} band was shifted to 1168.2 cm^{-1} for the D_2O sample and gave an isotopic H/D ratio of 1.3798; the deuterium counterpart of the 1646.8 cm^{-1} band was overlapped by the D_2O absorptions. Accordingly, the 1010.5, 1611.9, and 1646.8 cm^{-1} bands are assigned to the Ti−O, antisymmetric, and symmetric TiH$_2$ stretching vibrations of the H$_2$TiO molecule.

The H$_2$TiO assignment receives further support from DFT calculations. As has been mentioned, the H$_2$TiO molecule was predicted to have a ^{1}A$'$ ground state and is slightly lower in energy than the inserted HTiOH molecule. The Ti−O and TiH$_2$ stretching vibrations were predicted to be 1082, 1690, and 1730 cm^{-1}, which require scaling factors of 0.934, 0.953, and 0.952 to fit the observed values.

As with the titanium example, zirconium reacted with water to give the H$_2$ZrO. The formation of this species is confirmed by absorptions at 1577.6 and 1539.4, and four bands at 924.7, 923.9, 923.1, and 921.6 cm^{-1}. These bands can be grouped together by noting their consistent behavior upon annealing and photolysis. The relative intensities of the 924.7, 923.9, 923.1, and 921.6 cm^{-1} bands matched those of natural isotopic abundance zirconium and clearly indicate involvement of one Zr atom. In the reactions of Zr with the $H_2^{16}O + H_2^{18}O$ mixture, these four bands split into four spaced doublets, while in the mixed $H_2O + HDO + D_2O$ experiment, a very closely spaced triplet with and intermediate at 923.8 cm^{-1} was clearly observed for the most intense 924.7 cm^{-1} band. The deuterium and oxygen shifts and splittings indicate that two equivalent hydrogen atoms and one oxygen atom are involved in this molecule. The 1577.6 and 1539.4 cm^{-1} bands gave deuterium counterparts at 1130.3 and 1107.8 cm^{-1} and defined H/D ratios

Figure 9. B3LYP-calculated geometric parameters (bond lengths in angstroms; bond angles in degrees) and relative stability (kilocalories per mole) of the H$_2$MO and HMOH isomers.

Table 7. Calculated Vibrational Frequencies (cm^{-1}) and Intensities (km/mol) for the Structures Described in Figure 9

molecule	frequency (intensity)
H$_2$TiO (^{1}A$'$)	1730 (170), 1690 (465), 1082 (271), 636 (91), 536 (7), 427 (235)
HTiOH (^{3}A$''$)	3922 (158), 1591 (392), 721 (188), 464 (151), 448 (211), 304 (133)
HTiOH (^{1}A$'$)	3931 (306), 1674 (379), 779 (174), 401 (27), 346 (160), 269 (177)
H$_2$ZrO (^{1}A$'$)	1662 (180), 1620 (461), 942 (220), 590 (114), 528 (11), 457 (153)
HZrOH (^{3}A$''$)	3935 (209), 1577 (403), 679 (151), 414 (157), 407 (162), 323 (87)
HZrOH (^{1}A$'$)	3933 (298), 1680 (264), 717 (103), 404 (113), 379 (128), 276 (50)
H$_2$HfO (^{1}A$'$)	1714 (138), 1683 (338), 932 (182), 663 (70), 549 (9), 498 (131)
HHfOH (^{3}A$''$)	3968 (219), 1601 (314), 683 (117), 420 (140), 409 (162), 265 (52)
HHfOH (^{1}A$'$)	3942 (230), 1679 (312), 708 (87), 523 (110), 512 (132), 317 (27)

of 1.3957 and 1.3896, respectively. In the mixed $H_2O + HDO + D_2O$ experiments (Figure 5), two additional bands at 1558.0 and 1119.2 cm^{-1} were observed; these two bands are due to Zr−H and Zr−D stretching vibrations of the HDZrO molecule.

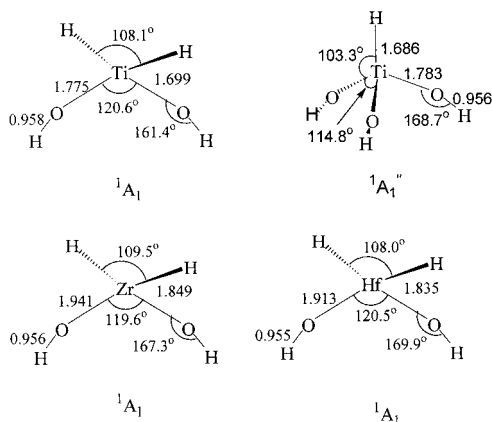B3LYP calculations predicted a ^{1}A$'$ ground-state H$_2$ZrO molecule with ZrH$_2$ and Zr−O stretching vibrations at 1662, 1620, and 942 cm^{-1}, which require scaling factors of 0.949, 0.950, and 0.982 to fit the observed frequencies. Of more importance, the calculated isotopic shifts and splittings are reproduced to substantial accuracy (−8.8, −0.5, and +0.2 cm^{-1} for D$_2$ZrO, +0.4, +1.9, and −0.2 cm^{-1} for HDZrO), which adds further support to the assignment.

Similar bands at 1646.4, 1615.6, and 921.0 cm^{-1} in the Hf + H$_2$O experiments are assigned to the H$_2$HfO molecule following the examples of the H$_2$TiO and H$_2$ZrO molecules. DFT calculations predicted that the H$_2$HfO molecule also has a ^{1}A$'$ ground state, with the three above modes at 1714, 1683, and 932 cm^{-1}.

HMOH. In the previous thermal Ti atom and water reaction study,[6] two bands at 1538.9 and 699.7 cm^{-1} were been assigned to the Ti−H and Ti−OH stretching vibrational modes of the inserted HTiOH molecule. In the present experiments, a weak band at 1549.1 cm^{-1} appeared on annealing and was destroyed on photolysis when H$_2$TiO absorptions were greatly enhanced. This band is assigned to the Ti−H stretching vibration of the

Table 8. Calculated Vibrational Frequencies (cm^{-1}) and Intensities (km/mol) of the Structures Described in Figure 10

	sym-O–H	asym-O–H	sym-M–H	asym-M–H	sym-M-OH	asym-M-OH
H$_2$Ti(OH)$_2$	3952 (258)	3948 (339)	1773 (206)	1741 (411)	777 (154)	852 (342)
H$_2$Zr(OH)$_2$	3971 (217)	3968 (343)	1685 (257)	1649 (506)	708 (161)	737 (355)
H$_2$Hf(OH)$_2$	3995 (194)	3992 (351)	1729 (226)	1694 (431)	720 (159)	717 (303)

Figure 10. B3LYP-calculated geometric parameters (bond lengths in angstroms; bond angles in degrees) of the H$_2$M(OH)$_2$ and HTi(OH)$_3$ molecules.

Table 9. Observed and Calculated Isotopic Frequency Ratios of the HMO and H$_2$MO Molecules

		H/D		^{16}O/^{18}O	
		obsd	calcd	obsd	calcd
H$_2$TiO	sym-TiH		1.4040	1.0009	1.0001
	asym-TiH	1.3798	1.3905	1.0004	1.0000
	Ti–O	1.0009	1.0023	1.0430	1.0431
H$_2$ZrO	sym-ZrH	1.3957	1.4067	1.0000	1.0000
	asym-ZrH	1.3896	1.4024	1.0000	1.0000
	Zr–O	1.0025	1.0022	1.0494	1.0499
H$_2$HfO	sym-HfH		1.0494	1.0000	1.0000
	asym-HfH	1.3950	1.4081	1.0000	1.0000
	Hf–O	1.0025	1.0025	1.0540	1.0544
HTiO	Ti–H	1.3848	1.3969	1.0003	1.0001
	Ti–O	1.0009	1.0008	1.0439	1.0441
HZrO	Zr–H	1.3915	1.4050	1.0000	1.0000
	Zr–O	1.0015	1.0007	1.0498	1.0506
HHfO	Hf–H		1.4087	1.0000	1.0000
	Hf–O	1.0022	1.0009	1.0553	1.0551

HTiOH molecule. The present DFT calculations predicted a ^{3}A″ ground-state HTiOH with bent geometry; the Ti–H and Ti–OH stretching vibrational modes were calculated at 1591.2 and 721.0 cm^{-1} for 392:188 relative intensities. Our spectrum below the 700 cm^{-1} region is noisy, and the Ti–OH mode was not observed in our experiments.

A weak band at 1530.9 cm^{-1} in the Zr + H$_2$O experiments also appeared on annealing and was destroyed on photolysis. The deuterium counterpart at 1098.2 cm^{-1} defines a 1.3940 H/D ratio. This band is assigned to the Zr–H stretching mode of the HZrOH molecule. Calculations predict this mode at 1577 cm^{-1} for the ^{3}A″ ground-state HZrOH molecule. The Zr–OH stretching mode was calculated at 679 cm^{-1} with much lower intensity and was not observed.

There is no evidence for the HHfOH molecule. DFT calculations indicate that the HHfOH molecule has a ^{1}A′ ground state with a Hf–H stretching vibration at 1679 cm^{-1}.

H$_2$M(OH)$_2$. Four bands at 1688.3, 1666.2, 805.5, and 775.5 cm^{-1} grew in together on annealing, suggesting different modes of the same molecule. These bands were also observed in previous thermal atom reactions[6] and were favored in high water concentration experiments, suggesting that this molecule may result from reaction of more than one water molecule. These four bands are assigned to the TiH$_2$ and Ti–(OH)$_2$ stretching vibrations of the H$_2$Ti(OH)$_2$ molecule. Absorptions at 1604.6, 1596.5, 707.3, and 660.1 cm^{-1} in the Zr + H$_2$O experiments, and at 1675.8, 1665.3, 690.7, and 660.4 cm^{-1} in the Hf + H$_2$O experiments, exhibited behavior very similar to that of the H$_2$Ti(OH)$_2$ absorptions and are assigned to the analogous H$_2$Zr(OH)$_2$ and H$_2$Hf(OH)$_2$ molecules.

The H$_2$M(OH)$_2$ assignments were further supported by DFT calculations. As listed in Figure 10, all three H$_2$M(OH)$_2$ molecules were predicted to have a ^{1}A$_1$ ground state and C_{2v} symmetry with the MH$_2$ plane perpendicular to the M(OH)$_2$ plane. As can be seen in Table 8, the calculated symmetric and antisymmetric MH$_2$ and M–(OH)$_2$ stretching vibrations are in good agreement with the observed values.

Other Absorptions. In the Ti + H$_2$O experiments, two weak bands at 1341.8 and 933.4 cm^{-1}, present on sample deposition, were destroyed on broadband photolysis with a 410 nm long-

wavelength pass filter and cannot be reproduced on further annealing, which suggests an anion assignment. In general, detaching electrons from negatively charged species requires little energy, and easy photolysis by near-infrared or visible radiation may suggest that the carrier is an anion. Cations are usually easy to destroy by UV radiation.[39] The upper band shifted to 1071.0 cm^{-1} for the D$_2$O sample, and the H/D isotopic ratio of 1.3716 indicates that this band is a Ti–H stretching vibration. The lower band exhibited a very small (2.3 cm^{-1}) deuterium isotopic shift and a large oxygen isotopic shift (37.6 cm^{-1}). These two bands are assigned to the Ti–H and Ti–O stretching vibrations of the HTiO$^-$ anion. DFT calculations predicted the HTiO$^-$ anion to have a ^{3}A″ ground state with bent geometry (∠HTiO, 119.7°; Ti–H, 1.856 Å; Ti–O, 1.660 Å). The Ti–H and Ti–O stretching vibrations were predicted to appear at 1347 and 940 cm^{-1}.

In the Ti + H$_2$O experiments, a 844.3 cm^{-1} band appeared on annealing; this band was favored in higher water concentration experiments. This band was also observed in previous thermal atom experiments and was tentatively assigned to Ti(OH)$_x$, with x = 3 or 4.[6] In the experiments reported in ref 6, a quartet was clearly resolved in the mixed H$_2$O + H$_2^{18}$O spectrum, indicating that three equivalent oxygen atoms are involved. In the present study, a weak band in the Ti–H stretching vibrational frequency region at 1634.3 cm^{-1} went together with the 844.3 cm^{-1} band, suggesting different modes of the same molecule. These two bands are assigned to the Ti–H and Ti–OH stretching vibrations of the HTi(OH)$_3$ molecule. The HTi(OH)$_3$ molecule was calculated to have a ^{1}A$_1$″ ground state with C_{3v} symmetry (Figure 10), a strong doubly degenerate Ti–OH stretching vibration at 816 cm^{-1}, and a slightly weaker Ti–H stretching vibration at 1777 cm^{-1}.
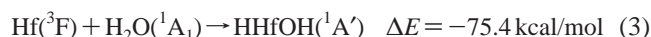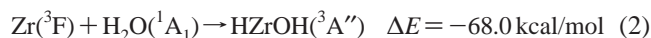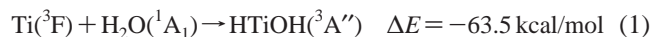
In all three systems, weak MO$_2$ absorptions were observed (TiO$_2$, 917.0 cm^{-1}; ZrO$_2$, 818.0 cm^{-1}; HfO$_2$, 813.9 cm^{-1}).[35] These absorptions exhibited no shift when the isotopic H$_2^{18}$O sample was used, suggesting that the MO$_2$ molecules might be produced from a trace of O$_2$ impurity in the system.

(39) Bondybey, V. E.; Smith, A. M.; Agreiter, J. *Chem. Rev.* **1996**, *96*, 2113.
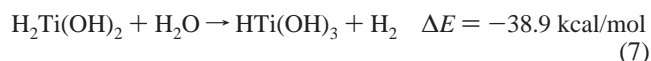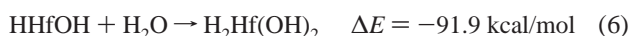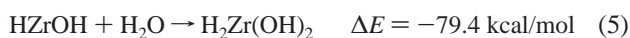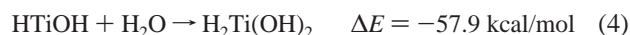
Table 9 compares the observed and calculated isotopic vibrational frequency ratios of the major product HMO and H_2MO molecules. The observed ratios are in good agreement with the calculated ratios, indicating that the present DFT calculations predicted the normal modes correctly.

Reaction Mechanism. Co-condensation of laser-ablated Ti and Zr atoms with water molecules in excess argon at 11 K resulted in the formation of the insertion product HTiOH and HZrOH molecules; however, there is no evidence of the HHfOH molecule. Our theoretical calculations indicated that all three insertion reactions (1)−(3) are exothermic (B3LYP values).

$$Ti(^3F) + H_2O(^1A_1) \rightarrow HTiOH(^3A'') \quad \Delta E = -63.5 \, \text{kcal/mol} \quad (1)$$

$$Zr(^3F) + H_2O(^1A_1) \rightarrow HZrOH(^3A'') \quad \Delta E = -68.0 \, \text{kcal/mol} \quad (2)$$

$$Hf(^3F) + H_2O(^1A_1) \rightarrow HHfOH(^1A') \quad \Delta E = -75.4 \, \text{kcal/mol} \quad (3)$$
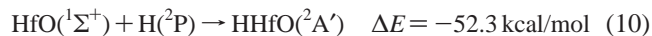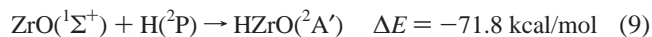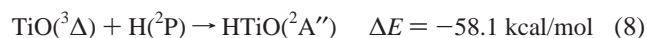
However, both HTiOH and HZrOH molecules have triplet ground states, while HHfOH has a singlet ground state, so reactions (1) and (2) conserve spin, while there is spin crossing for reaction (3). As will be discussed, there is no spin crossing from $HHfOH(^1A')$ to $H_2HfO(^1A')$, and this suggests that HHfOH is very short-lived, rapidly rearranging to form the H_2HfO molecule.

The $H_2M(OH)_2$ and $HTi(OH)_3$ absorptions increased on annealing, suggesting that HMOH molecules can further react with water via reactions (4)−(7). These reactions were calculated to be exothermic (B3LYP values).

$$HTiOH + H_2O \rightarrow H_2Ti(OH)_2 \quad \Delta E = -57.9 \, \text{kcal/mol} \quad (4)$$

$$HZrOH + H_2O \rightarrow H_2Zr(OH)_2 \quad \Delta E = -79.4 \, \text{kcal/mol} \quad (5)$$

$$HHfOH + H_2O \rightarrow H_2Hf(OH)_2 \quad \Delta E = -91.9 \, \text{kcal/mol} \quad (6)$$

$$H_2Ti(OH)_2 + H_2O \rightarrow HTi(OH)_3 + H_2 \quad \Delta E = -38.9 \, \text{kcal/mol} \quad (7)$$

The formation of MO and HMO species on sample deposition indicates that part of the HMOH molecules formed in the gas phase are dissociated to HMO, MO, and H_2 or H during deposition. Laser ablation of the metal target produces ground-state atoms as well as excited atoms. The excited metal atom reactions may give contributions to the formation of these products. There is no evidence of the MH and MOH molecules.[1] The HMO absorptions increased on annealing, suggesting that HMO molecules can also be formed by reactions of MO and H atoms.

$$TiO(^3\Delta) + H(^2P) \rightarrow HTiO(^2A'') \quad \Delta E = -58.1 \, \text{kcal/mol} \quad (8)$$

$$ZrO(^1\Sigma^+) + H(^2P) \rightarrow HZrO(^2A') \quad \Delta E = -71.8 \, \text{kcal/mol} \quad (9)$$

$$HfO(^1\Sigma^+) + H(^2P) \rightarrow HHfO(^2A') \quad \Delta E = -52.3 \, \text{kcal/mol} \quad (10)$$

The HTiOH absorptions were destroyed on broadband photolysis, and two reaction paths were observed: rearrangement to form the H_2TiO isomer and H_2 elimination to form TiO + H_2. For the Zr and Hf + H_2O systems, the H_2ZrO and H_2HfO absorptions increased on annealing, and the ZrO and HfO absorptions were not enhanced on broadband photolysis. In previous thermal Ti atom experiments, H_2TiO (which was incorrectly assigned as TiO) was observed on sample deposition; as the authors discussed, light from the hot furnace walls may be capable of photolyzing the HTiOH molecules.[6]
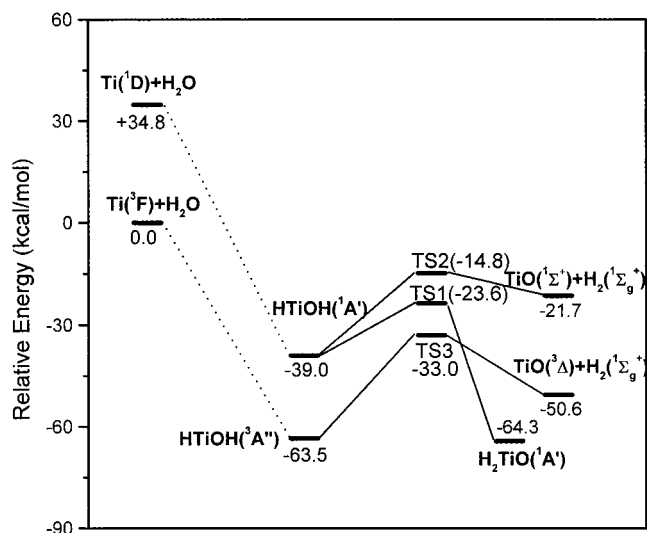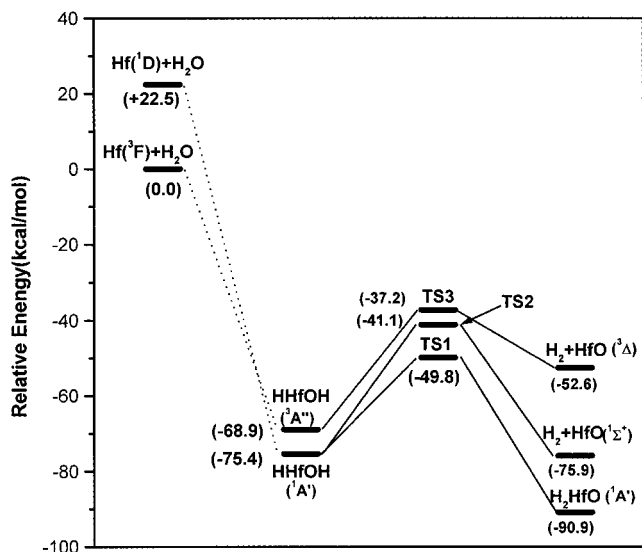

Figure 11. Potential energy surface for the Ti + H_2O reaction at the B3LYP level. Energies given are in kilocalories per mole and are relative to the separated ground-state reactants: $Ti(^3F) + H_2O(^1A_1)$. The dashed lines indicate areas unexplored computationally.
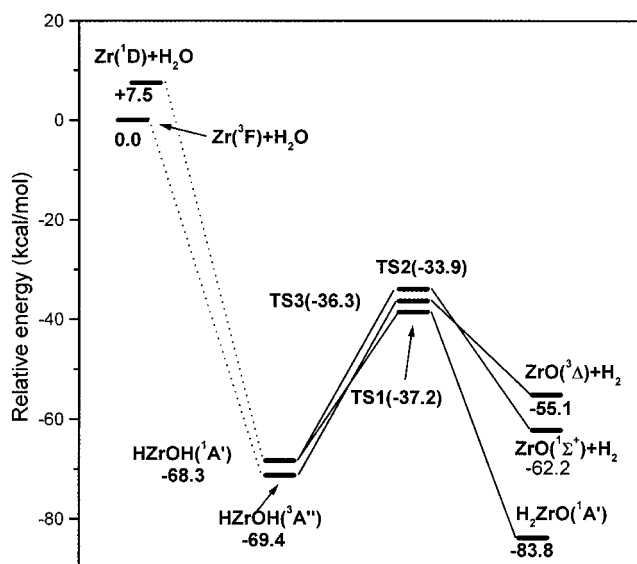
Figure 12. Potential energy surface for the Zr + H_2O reaction at the CCSD(t) level. Energies given are in kilocalories per mole and are relative to the separated ground-state reactants: $Zr(^3F) + H_2O(^1A_1)$. The dashed lines indicate areas unexplored computationally.

Figures 11−13 show qualitative singlet and triplet potential energy surfaces for the Ti, Zr, and Hf + H_2O reaction systems. For the Ti and Hf systems, the relative stabilities of all species calculated at the B3LYP and CCSD(t) levels are the same, so the B3LYP calculation results were used for plots, but for the Zr system, the B3LYP calculations predicted the relative stability of $^3\Delta$ and $^1\Sigma^+$ states of ZrO in error, so the CCSD(t) results were used. In all three systems, there is no evidence of a metal atom−water molecule adduct, and the present DFT calculations failed to find true minima for such metal−water complexes. Thus, the initial interaction is assumed to be direct metal atom insertion into a HO−H bond to form the insertion HMOH molecule. The ^3F ground-state Hf is seen to exhibit spin-forbidden crossing, leading to low-spin HHfOH; however, neither $Ti(^3F)$ nor $Zr(^3F)$ exhibits spin crosssing.

From HMOH, two reaction paths are possible on the singlet surface. One path is the hydrogen transfer from oxygen to the

Figure 13. Potential energy surface for the Hf + H_2O reaction at the B3LYP level. Energies given are in kilocalories per mole and are relative to the separated ground-state reactants: Hf(^{3}F) + H_2O($^1A_1$). The dashed lines indicate areas unexplored computationally.

metal center to form H_2MO through transition state 1 (TS1). This process involves the breaking of the O—H bond and the formation of a M—H σ bond and a M—O π bond. The other path is the hydrogen transfer from oxygen to hydrogen through transition state 2 (TS2). This transition state leads to H_2 elimination to form the monoxides. This process involves the breaking of the H—O bond and one covalent M—H bond, with the formation of the H—H bond and a M—O π bond. On the triplet surface, there is only the H_2 elimination path through transition state 3 (TS3), as no stable triplet H_2MO was found. The calculated structural parameters of the aforementioned transition states are shown in Figure 14.

In the case of Ti, both the HTiOH and TiO have triplet ground states. The transition state 3 from HTiOH(^{3}A″) to TiO(^{3}Δ) lies lower in energy than the transition state 1 from HTiOH(^{1}A′) to H_2TiO(^{1}A′), and there is spin crossing leading to the H_2TiO-(^{1}A′) product. In the case of Zr, the HZrOH also has a triplet ground state with the singlet very closely in energy. There also exists spin crossing from HZrOH(^{3}A″) to H_2ZrO(^{1}A′). Unlike TiO, ZrO has a singlet ground state, formation of ZrO($^1\Sigma^+$) from HZrOH (^{3}A″) also requires spin crossing, and the transition state 3 lies higher in energy than the transition state 1, which makes the formation of ZrO($^1\Sigma^+$) unfavorable. In the case of Hf, both HHfOH and HfO have singlet ground states, and the formations of both H_2HfO(^{1}A′) and HfO($^1\Sigma^+$) require no spin crossing. As transition state 1 (leading the formation of H_2HfO) lies lower in energy than transition state 2 (leading the formation of HfO), the formation of H_2HfO dominates the reaction.

The results on the Ti + H_2O system are different from those for the Sc + H_2O system.[20] As Sc has only three valence electrons, there are not enough electrons to satisfy chemical bonding in H_2ScO, so the H_2ScO species is unstable. The only reaction path of HScOH is the H_2 elimination process to form
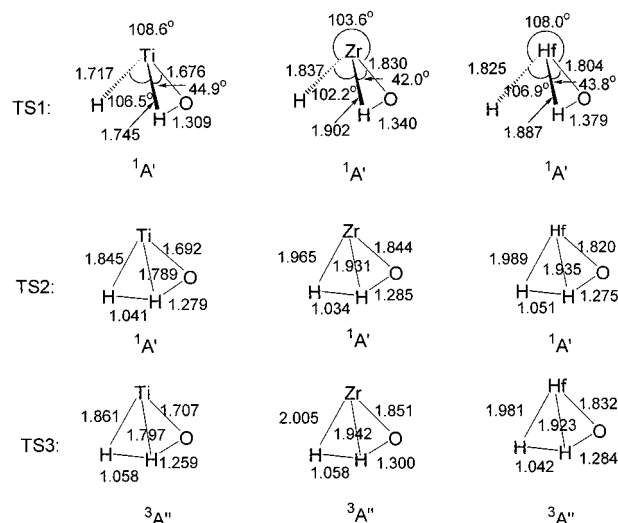
Figure 14. B3LYP-calculated geometric parameters (bond lengths in angstroms; bond angles in degrees) of the transition states.

the ScO. As V atom has five valence electrons, chemical bonding in H_2VO can also be satisfied. Similar to Ti, both the H_2VO and VO formation paths are observed in the V + H_2O reaction.[40] However, the H_2MO^+ (M = Sc, Ti, V) intermediates in the M^+ + H_2O reactions are quite different: there is no M—H covalent bond, and these H_2MO^+ species can be viewed as ion—molecule complexes.[17,18]

Conclusions

The reactions of Ti, Zr, and Hf atoms with water molecules have been investigated using the laser ablation technique and theoretical calculations. The metal atoms reacted with water molecules to form the insertion products HMOH and $H_2M(OH)_2$ spontaneously on annealing in solid argon. Two photon-induced reaction paths were observed for HTiOH: rearrangement to form the H_2TiO isomer and H_2 elimination to form the monoxide TiO. In the cases of Zr and Hf, the H_2ZrO and H_2HfO molecules were produced on annealing spontaneously, but the H_2 elimination to form the monoxide process was not observed on photolysis. In addition, the HMO species were also observed and identified.

The excellent agreement with frequencies and isotopic frequency shifts from density functional calculations strongly support the assignments of the aforementioned species. In addition, qualitative analysis of the reaction paths leading to the observed products are given, including several important transition states.

(40) Zhang, L. N.; Dong, J.; Zhou, M. F.; Qin, Q. Z., manuscript in preparation.